

Facial Performance Capture with Deep Neural Networks

Samuli Laine
NVIDIA

Tero Karras
NVIDIA

Timo Aila
NVIDIA

Antti Herva
Remedy Entertainment

Jaakko Lehtinen
NVIDIA
Aalto University

Abstract

We present a deep learning technique for facial performance capture, i.e., the transfer of video footage into a motion sequence of a 3D mesh representing an actor’s face. Specifically, we build on a conventional capture pipeline based on computer vision and multi-view video, and use its results to train a deep neural network to produce similar output from a monocular video sequence. Once trained, our network produces high-quality results for unseen inputs with greatly reduced effort compared to the conventional system.

In practice, we have found that approximately 10 minutes worth of high-quality data is sufficient for training a network that can then automatically process as much footage from video to 3D as needed. This yields major savings in the development of modern narrative-driven video games involving digital doubles of actors and potentially hours of animated dialogue per character.

1 Introduction

Using digital doubles of human actors is a key component in modern video games’ strive for realism. Transferring the essence of a character into digital domain has many challenging technical problems, but the accurate capture of facial movement remains especially tricky. Due to humans’ innate sensitivity to the slightest facial cues, it is difficult to surpass the uncanny valley, where an otherwise believable rendering of a character appears lifeless or otherwise unnatural.

Various tools are available for building facial capture pipelines that take video footage into 3D in one form or another, but their accuracy leaves room for improvement. In practice, high-quality results are generally achievable only with significant amount of manual polishing of output data. This can be a major cost in a large video game production. Furthermore, the animators doing the fixing need to be particularly skilled, or otherwise this editing may introduce distracting, unnatural motion.

In this paper, we introduce a neural network based solution to facial performance capture. Our goal is not to remove the need for manual work entirely, but to dramatically reduce the extent to which it is required. In our approach, a conventional capture pipeline needs to be applied only to a small subset of input footage, in order to generate enough data for training a neural network. The bulk of the footage can then be processed using the trained network, skipping the conventional labor-intensive capture pipeline entirely. Our approach is outlined in Figure 1.

1.1 Problem statement

We assume that the input for the capture pipeline is one or more video streams of the actor’s head captured under controlled conditions. The positions of the cameras remain fixed, the lighting and background are standardized, and the actor is to remain at approximately the same position relative to the cameras throughout all shots. Naturally, some amount of movement needs to be allowed, and we achieve this through input data augmentation in the training phase (Section 4.1).

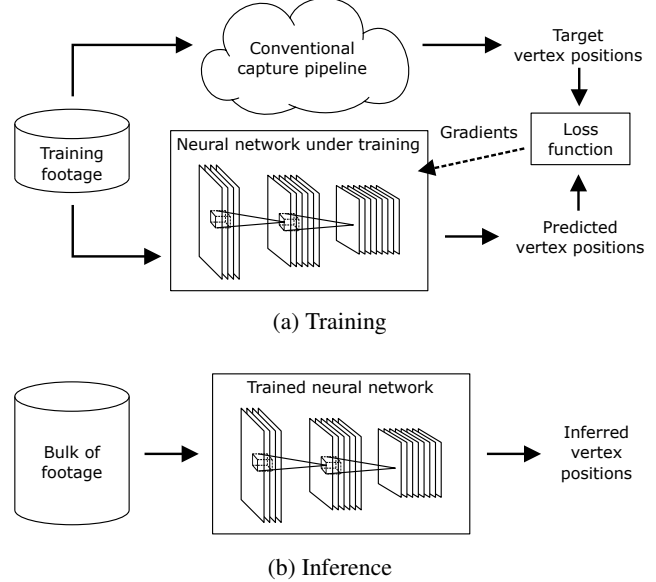


Figure 1: The goal of our system is to reduce the amount of footage that needs to be processed using a conventional, labor-intensive capture pipeline. (a) In order to train a neural network, all training footage must be processed using a conventional capture pipeline. This provides the input/target pairs that are necessary for the network to learn how to perform the mapping from video footage to vertex positions. According to our experiments, approximately 10 minutes worth of training material is sufficient per actor. (b) For processing the bulk of the material, the conventional capture pipeline can be skipped. Depending on the amount of material, this can yield significant cost savings in production.

In our case, the outputs of the capture pipeline are the per-frame positions of the control vertices of a facial mesh, as illustrated in Figure 2. There are various other ways to encode the facial expression, including rig parameters or blend shape weights. In the system where our network was developed in, those kind of encodings are introduced in later stages, mainly for compression and rendering purposes, but the primary capture output consists of the positions of approximately 5000 animated vertices on a fixed-topology facial mesh.

1.2 Existing capture pipeline at Remedy

Target data necessary for training the neural network was generated using Remedy Entertainment’s existing capture pipeline based on the commercial DI4D PRO system [Dimensional Imaging 2016] that employs nine video cameras. The benefit of this system is that it captures the nuanced interactions of the skull, muscles, fascia and skin of an actor so as to bypass complex and expensive facial rigging and tissue simulations for digital doubles.

First an unstructured mesh with texture and optical flow data is cre-

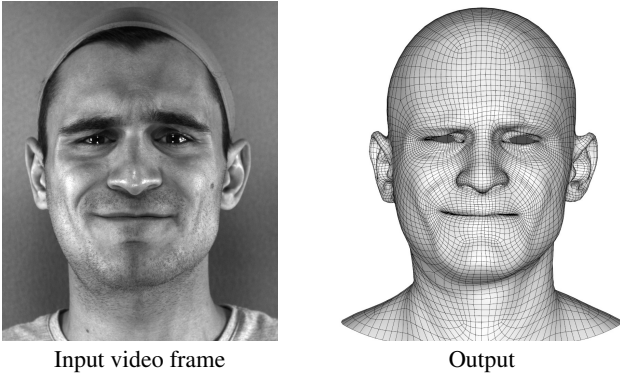


Figure 2: Input for the conventional capture pipeline is a set of nine images, whereas our network only uses a cropped portion of the center camera image converted to grayscale. Output of both the conventional capture pipeline and our network consists of the 3D positions of ~ 5000 animated control vertices for each frame.

ated from the images for each frame of a facial performance. A fixed-topology template mesh, created prior to the capture work using a separate photogrammetry pipeline, is then projected on to the unstructured mesh and associated with the optical flow. The template mesh is tracked across the performance and any issues are fixed semi-automatically in the DI4DTrack software by a tracking artist. The position and orientation of the head are then stabilized using a few key vertices of the tracking mesh. Finally a point cache of the facial performance is exported for the fixed-topology template mesh. The point cache file contains the positions of each vertex in the mesh for each frame of animation in the shot.

Additional automated deformations are later applied to the point cache to fix the remaining issues. These deformations were not applied to the point caches in the training set. For example, the eyelids are deformed to meet the eyeball exactly and to slide slightly with motion of the eyes. Also, opposite vertices of the lips are smoothly brought together to improve lip contacts when needed. After animating the eye directions the results are compressed for runtime use in Remedy’s Northlight engine using 416 facial joints. Pose space deformation is used to augment the facial animation with detailed wrinkle normal map blending.

2 Previous Work

While facial performance capture systems come in many varieties, all share a fundamental goal: the non-rigid tracking of the shape of the actor’s head throughout a performance, given inputs in the form of video sequences, RGB-D sequences, or other measurements. Once solved for, the moving geometry is often further retargeted onto an existing animation rig for further processing. In this work, we concentrate on the first problem: given a video sequence as input, our system outputs a time-varying mesh sequence that tracks the performance.

There are numerous existing methods for time-varying facial 3D reconstruction (tracking). Markers drawn at specific locations on the actor’s face enable multi-view stereo techniques to find the markers’ trajectories in space, and knowledge of their positions on the face geometry allow estimating a deformation for the entire head [Williams 1990]. Markerless techniques, on the other hand, attempt to track the entire face simultaneously, often with the help of a parameterized template head model that may include animation priors, e.g., [Zhang et al. 2004; Weise et al. 2011], or by performing multi-view stereo or photometric reconstructions of the individual

input frames [Furukawa and Ponce 2009; Beeler et al. 2011; Fyffe et al. 2011].

In contrast to the direct geometric computer vision approaches described above, machine learning techniques have been successfully applied to facial performance capture as well. A typical approach is to use radial basis functions (RBF) to infer blend-shape weights from motion-capture data based on a set of training examples [Deng et al. 2006]. More recently, restricted Boltzmann machines (RBM) and multi-layer perceptrons (MLP) have also been used for similar tasks [Zeiler et al. 2011; Costigan et al. 2014]. Furthermore, neural networks have been used to infer facial animation data from audio [Hong et al. 2002]. To our knowledge, none of the existing machine learning methods are, however, able to perform facial performance capture from video data in an end-to-end fashion. As a consequence, they have to rely on other techniques to extract time-varying feature vectors from the video.

We base our work on deep convolutional neural networks [Simard et al. 2003], which have received significant attention in the recent years and proven particularly well suited for large-scale image recognition tasks [Krizhevsky et al. 2012; Simonyan and Zisserman 2014]. Modern convolutional neural networks employ various techniques to reduce training time and improve generalization over novel input data. These include piecewise-linear activation functions [Krizhevsky et al. 2012], data augmentation [Simard et al. 2003], dropout regularization [Hinton et al. 2012; Srivastava et al. 2014], and GPU acceleration [Krizhevsky et al. 2012]. Furthermore, it has been shown that state-of-the-art performance can be achieved with a very simple network architecture that mainly consists of small 3×3 convolutional layers [Simonyan and Zisserman 2014] that employ strided output to reduce spatial resolution throughout the network [Springenberg et al. 2014].

In a way, our method is a “meta-algorithm” in the sense that it relies on an existing technique for generating the training examples; however, after our network has learned to mimic the host algorithm, it produces results at a fraction of the cost. While we base our system on a specific commercial solution, the same general idea can be built on top of any facial motion capture technique taking video inputs.

3 Network Architecture

Our input footage is divided into a number of shots, with each shot typically consisting of 100–2000 frames at 30 FPS. Data for each input frame consists of a 1200×1600 pixel image from each of the nine cameras. As explained above, the output is the per-frame vertex positions for each of the ~ 5000 facial mesh vertices, i.e., ~ 15000 scalars ($= N_{\text{out}}$) in total.

As the input for the network, we take the 1200×1600 video frame from the central camera, crop it with a fixed rectangle so that the face remains in the picture, and scale the remaining portion to 240×320 resolution. Furthermore, we convert the image to grayscale, resulting in a total of 76800 scalars to be fed to the network. The resolution may seem low, but numerous tests confirmed that increasing it did not improve the results.

During the course of the project, we experimented with two neural network architectures. Our initial efforts concentrated on a fully connected network, but it was soon discovered that a convolutional network architecture was better suited for the task. For the sake of completeness, we detail the fully connected network in Appendix B, where we also briefly characterize its strengths and weaknesses compared to the convolutional network.

3.1 Convolutional network

Our convolutional network is based on the all-convolutional architecture [Springenberg et al. 2014] extended with two fully connected layers to produce the full-resolution vertex data at output. The input is a whitened version of the 240×320 grayscale image. For whitening, we calculate the mean and variance over all pixels in the training images, and bias and scale the input so that these are normalized to zero and one, respectively.

Note that same whitening coefficients, fixed at training time, are used for all input images during training, validation, and production use. If the whitening were done on a per-image or per-shot basis, we would lose part of the benefits of the standardized lighting environment. For example, variation in the color of the actor’s shirt between shots would end up affecting the brightness of the face. The layers of the network are listed in the table below.

Name	Description
input	Input $1 \times 240 \times 320$ image
conv1a	Conv 3×3 , $1 \rightarrow 64$, stride 2×2 , ReLU
conv1b	Conv 3×3 , $64 \rightarrow 64$, stride 1×1 , ReLU
conv2a	Conv 3×3 , $64 \rightarrow 96$, stride 2×2 , ReLU
conv2b	Conv 3×3 , $96 \rightarrow 96$, stride 1×1 , ReLU
conv3a	Conv 3×3 , $96 \rightarrow 144$, stride 2×2 , ReLU
conv3b	Conv 3×3 , $144 \rightarrow 144$, stride 1×1 , ReLU
conv4a	Conv 3×3 , $144 \rightarrow 216$, stride 2×2 , ReLU
conv4b	Conv 3×3 , $216 \rightarrow 216$, stride 1×1 , ReLU
conv5a	Conv 3×3 , $216 \rightarrow 324$, stride 2×2 , ReLU
conv5b	Conv 3×3 , $324 \rightarrow 324$, stride 1×1 , ReLU
conv6a	Conv 3×3 , $324 \rightarrow 486$, stride 2×2 , ReLU
conv6b	Conv 3×3 , $486 \rightarrow 486$, stride 1×1 , ReLU
drop	Dropout, $p = 0.2$
fc	Fully connected $9720 \rightarrow 160$, linear activation
output	Fully connected $160 \rightarrow N_{\text{out}}$, linear activation

The output layer is initialized by precomputing a PCA basis for the output meshes based on the target meshes from the training data. Allowing 160 basis vectors explains approximately 99.9% of the variance seen in the meshes, which was considered to be sufficient. If we made the weights of the output layer fixed, i.e., made it a non-trainable layer, that would effectively train the remainder of the network to output the 160 PCA coefficients. However, we found that allowing the last layer to be trainable as well improved the results.

Note that if we merged the last two layers together, we would have a single $9720 \rightarrow N_{\text{out}}$ fully connected layer, which would have almost 40 times the number of trainable weights compared to the combination of two layers. Because 160 PCA basis vectors are sufficient for accurately covering the space of target meshes, these degrees of freedom would be unnecessary and only make the training more difficult and prone to overfitting.

The convolutional network, when trained with proper input augmentation (Section 4.1), is not sensitive to the position and orientation of the actor’s head in the input images. Hence no image stabilization is required as a pre-process.

It should be noted that the quality of the results is not overly sensitive to the exact composition of the network. Changing the geometric progression of the number of feature maps, removing some or all of the 1×1 stride convolution layers, or adding more such layers, did not substantially change the results. The architecture listed above was found to perform consistently well, and was possible to train in a reasonable time, so it was chosen for use in production. All results in this paper were computed using this architecture.

4 Training

For each actor, the training set consists of four parts, totaling approximately 10 minutes of footage. The composition of the training set is as follows.

Range of motion. In order to capture the maximal extents of the facial motion, a single range-of-motion shot is taken where the actor goes through a pre-defined set of extreme expressions. These include, e.g., opening the mouth as wide as possible, moving the jaw sideways and front as far as possible, pursing the lips, opening the eyes wide and forcing them shut, etc.

Expressions. Unlike the range-of-motion shot that contains exaggerated expressions, this set contains normal expressions such as squinting of the eyes, expression of disgust, etc. These kind of expressions must be included in the training set, as otherwise the network would not be able to replicate them in production use.

Pangrams. This set attempts to cover the set of possible facial motions during normal speech for a given target language, in our case English. The actor speaks one to three pangrams, i.e., sentences that are designed to contain as many different phonemes as possible, in several different emotional tones. A pangram fitting the emotion would be optimal but in practice this is not always feasible.

In-character material. This set leverages the fact that an actor’s performance of a character is often heavily biased in terms of emotional and expressive range for various dramatic and narrative reasons. This material is composed of the preliminary version of the script, or it may be otherwise prepared for the training. Only the shots that are deemed to support the different aspects of the character are selected so as to ensure that the trained network produces output that stays in character even if the inference isn’t perfect, or completely novel or out of character acting is encountered.

The composition of the training is typically roughly as follows: one minute of range-of-motion and expression shots, three minutes of pangrams across emotional states and up to six minutes of in-character performances of varying intensity and scenario. Natural delivery is preferred so as to ensure that the characteristics of the acting and the shoot as a session are reflected in the training set.

4.1 Data augmentation

We perform several transformations to the input images during training in order to make the network resistant to variations in input data. These transformations are executed on CPU concurrently with network evaluation and training that occurs on the GPU. Augmentation is not used when evaluating the validation loss or when processing unseen input data in production use. Examples of augmented input images are shown in Figure 3.

The main transformations are translation, rotation and zoom, which account for the motion of the actor’s head during capture. The magnitudes of these augmentations are set so that they cover at least all of the variation expected in the input data.

In addition to geometric transformations, we vary the brightness and contrast of the input images during training, in order to account for variations in lighting over the capture process. Our cameras pick a slight periodic flicker from the 50 Hz LED lights in the capture room, and it is possible that some of the bulbs degrade during the capture period that may take place over several days or weeks.

We also tried adding noise to the images, but this was found to be detrimental to learning, as was applying a variable gamma correction factor to approximate varying skin glossiness. Similarly, small

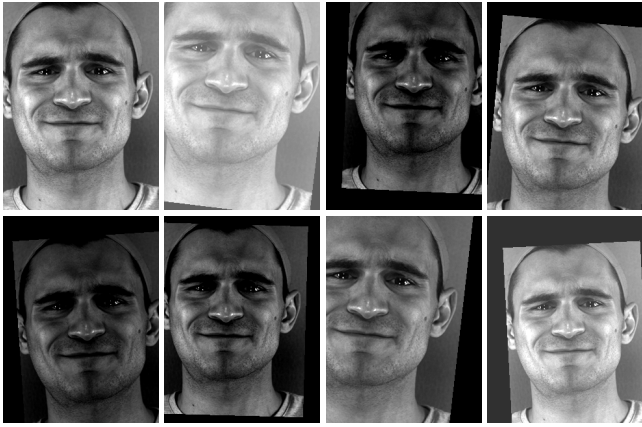


Figure 3: Examples of augmented inputs presented to the network during training. Top left image is the 240×320 crop from the same input video frame as was shown in Figure 2, and the remaining images are augmented variants of it.

2D perspective transformations—an attempt to crudely mimic the non-linear effects of rotations of the head—were not found to be beneficial.

4.2 Training parameters

We train the network for 200 epochs using the ADAM [Kingma and Ba 2014] optimization algorithm with parameters set to values recommended in the paper. The learning rate is ramped up using a geometric progression during the first training epoch, and then decreased according to $1/\sqrt{t}$ schedule. During the last 30 epochs we ramp the learning rate down to zero using a smooth curve, and simultaneously ramp ADAM β_1 parameter from 0.9 to 0.5. The ramp-up removes an occasional glitch where the network does not start learning at all, and the ramp-down ensures that the network converges to a local minimum. Minibatch size is set to 50, and each epoch processes all training frames in randomized order. Weights are initialized using the initialization scheme of He et al. [2015], except for the last output layer which is initialized using a PCA transformation matrix as explained in Section 3.1.

The strength of all augmentation transformations is ramped up linearly during the first five training epochs, starting from zero. This prevented a rare but annoying effect where the network fails to start learning properly, and gets stuck at clearly sub-optimal local minimum. The augmentation ramp-up process can be seen as a form of curriculum learning [Bengio et al. 2009].

Our loss function is simply the mean square error between the predicted vertex positions produced by the network and the target vertex positions in the training data. We experimented with a more complicated loss function (Appendix A.1), but did not find it useful in the end.

Our implementation is written in Python using Theano [Theano Development Team 2016] and Lasagne [Dieleman et al. 2015]. On a computer with a modern CPU and a NVIDIA GTX Titan X GPU, the training of one network with a typical training set containing 15000–18000 training frames ($\sim 8\text{--}10$ minutes at 30Hz) takes approximately 8–10 hours.

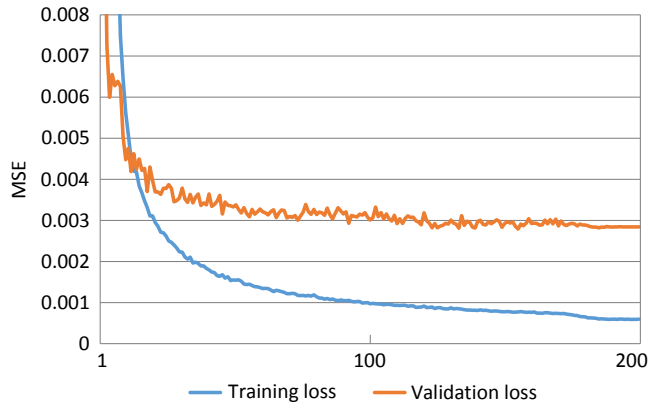


Figure 8: Convergence of the network during 200 training epochs. The effects of learning rate and β_1 rampdown can be seen in the final 30 epochs. This training run had ~ 15000 training frames and ~ 1800 validation frames, and took 8.25 hours to finish. This network was used for generating the outputs shown in Figures 4, 5 and 7.

5 Results and Discussion

Given the inevitable variability in the manual work involved in using the conventional capture pipeline, we could not hope that our network would reach a numerically exact match with manually prepared validation data. The goal of performance capture is to generate believable facial motion, and therefore the perceptual quality of the results—as judged by professional artists—is ultimately what decides whether a capture system is useful or not.

We shall first examine the numerical results, and then turn to perceptual results and production-related aspects that were learned during the project.

5.1 Numerical results

Figures 4 and 5 illustrate the accuracy of our trained network on a selection of interesting frames in two validation shots that were not used in training. Per-frame RMSE plot for the same validation shots is shown in Figure 6. We found that the neural network was very efficient in producing consistent output even when input data had variability due to inaccuracies of the conventional capture pipeline. As highlighted in Figure 5, the data obtained from the conventional capture pipeline sometimes contained systematic errors that the capture artists did not notice and thus correct. As long as overfitting is avoided, a neural network only learns the consistent features of the input-output mapping, and its output therefore does not fluctuate in the same way. We believe this explains some of the discrepancies between our output and the validation data.

Figure 7 demonstrates a problem with our decision to use only one input image as the input to the network: The single frontal image apparently does not contain enough information for the network to detect when the jaw is pushed to the front. We did not observe this issue until late in the project, and thus these errors need to be manually corrected when using our current system. We however expect that adding a secondary camera to the side of the actor and using both images as inputs to the network should correct this issue.

Figure 8 shows the convergence of the network that was used for creating the outputs in Figures 4, 5 and 7. As previously explained, our loss function is the MSE between network outputs and target positions from the training/validation set. The vertex coordinates

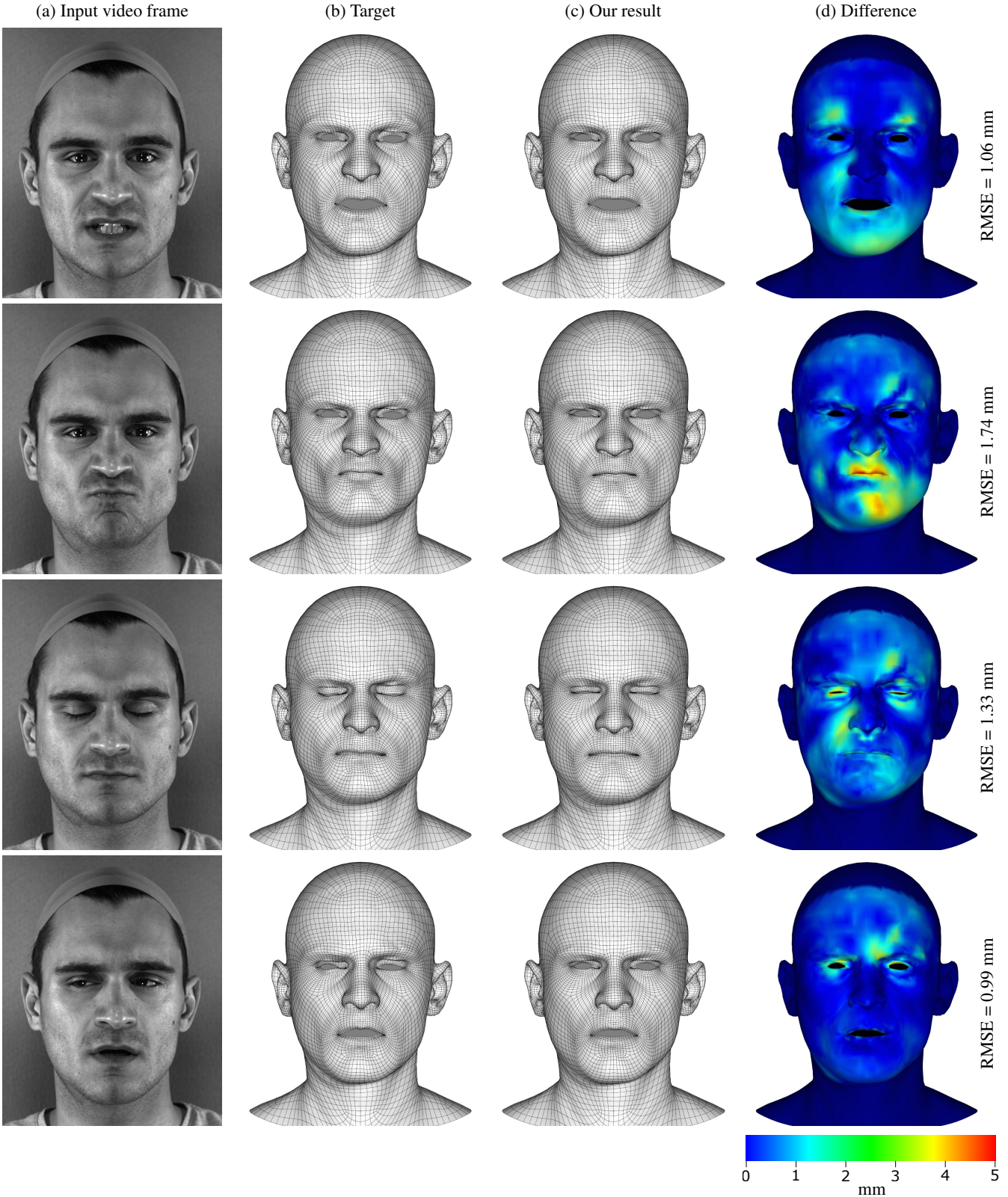


Figure 4: A selection of interesting frames from a validation shot that was not used as part of training set when training the network. (a) Crop of the original full-resolution input image. (b) The target positions were created by capture artists using the existing capture pipeline at Remedy Entertainment. (c) Our result, inferred by the neural network based solely on the input image (a). (d) Difference between target and inferred positions. The RMSE is calculated over the Euclidean distances between target and inferred vertex positions, with only the animated vertices taken into account. The RMSEs of these frames are higher than average, because the validation data mostly consist of more neutral material than the frames shown here.

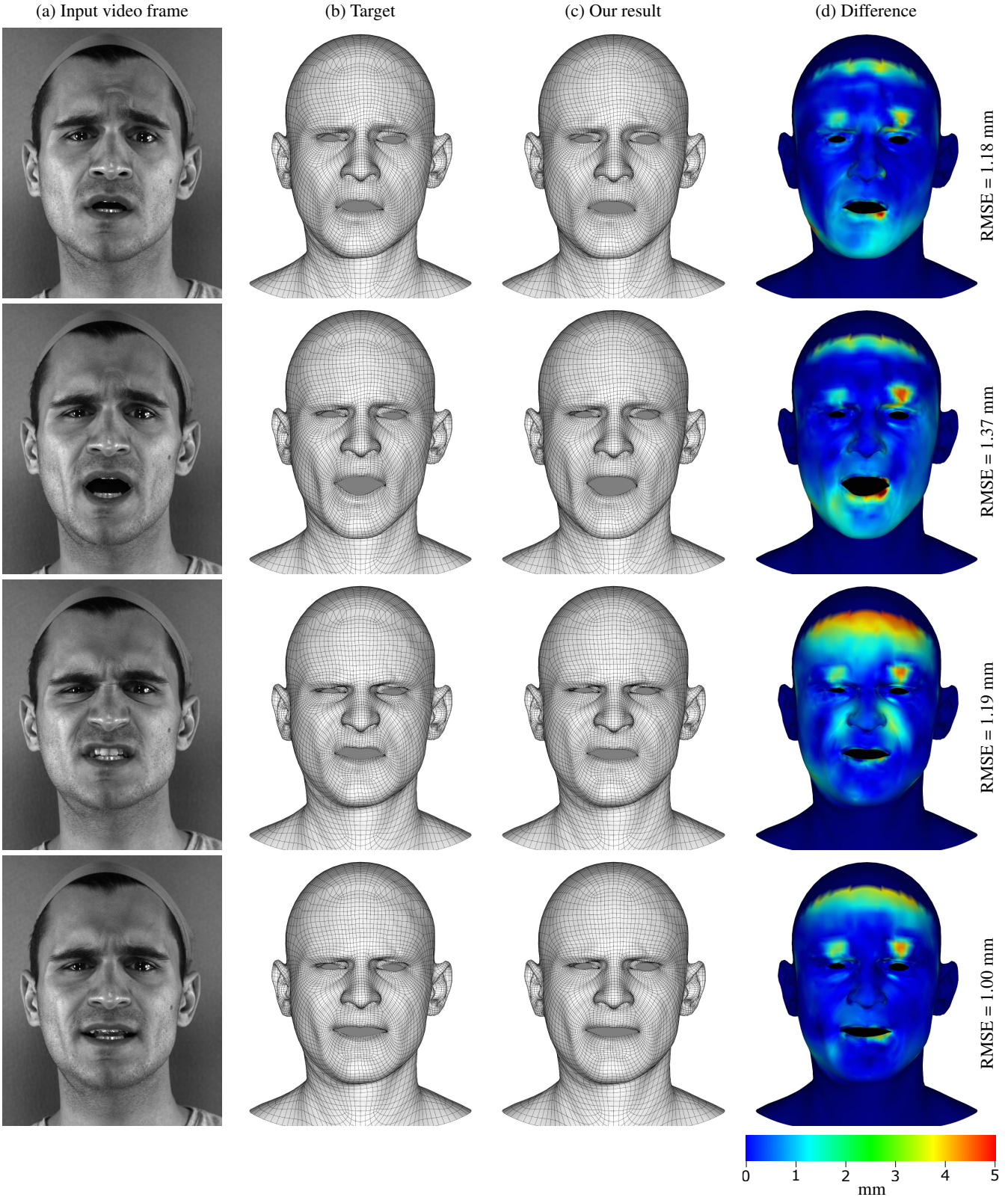


Figure 5: A selection of frames from another validation shot. Columns are as in Figure 4. Large differences are visible near the hairline, and these regions also appear distorted in the target meshes in column (b). It is not clear whether the manually tracked target positions or the inferred positions are closer to the ground truth. Because these regions have traditionally been problematic for the conventional capture pipeline, they are automatically smoothed with the stationary vertices of the head later in the animation pipeline, which corrects these issues. There are also two regions above the eyebrows that consistently show differences between inferred and target positions. It is likely that these are similarly due to a systematic tracking error in the target positions.

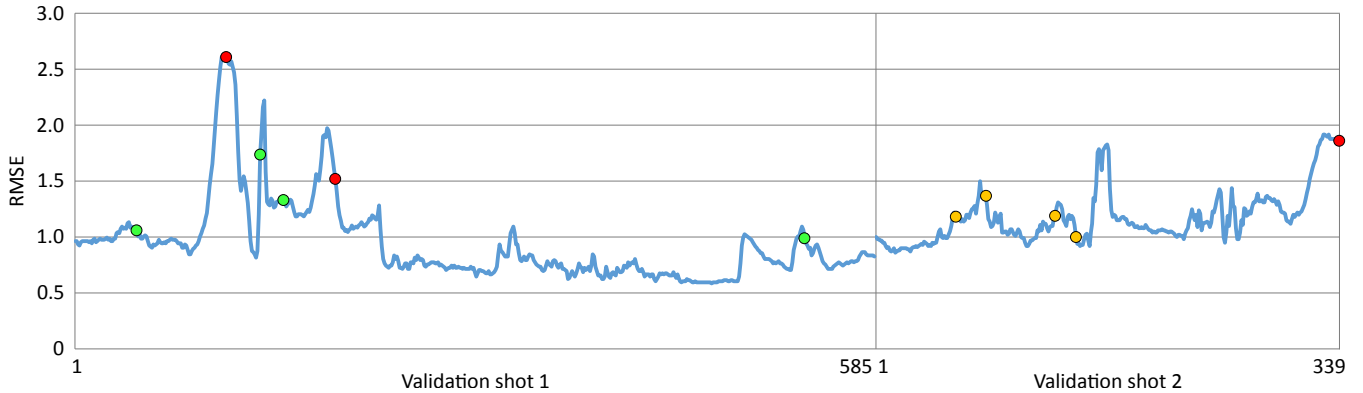


Figure 6: Per-frame RMSE in the two validation shots used for Figures 4 and 5. Frame index advances from left to right. The green dots indicate frames that were used in Figure 4, with leftmost dot corresponding to top row in Figure 4, etc. The orange dots indicate frames used in Figure 5, and the red dots indicate the problematic frames shown in Figure 7.

are measured in centimeters in our data, so the final validation loss of 0.0028 corresponds to RMSE of 0.92 millimeters. With longer training the training loss could be pushed arbitrarily close to zero, but this did not improve the validation loss or the subjective quality of the results.

The most unexpected result was that the network output was temporally perfectly stable, despite the fact that we do not employ recurrent networks or smooth the generated vertex positions temporally in any way.

5.2 Perceptual quality and production aspects

The original goal of the project was to cover the bulk of the facial tracking work specifically in facial performance heavy productions involving digital doubles of real actors, by inferring facial motion for non-cinematic parts of the game. The system is however currently being evaluated at Remedy Entertainment also for high-quality cinematic use, given the encouraging results.

The convolutional neural network was tested in the wild using footage from a later session. The lighting conditions and facial features exhibited in the training set were carefully preserved. The inference was evaluated numerically and perceptually in relation to a manually tracked ground truth. For extreme close-ups manual tracking still results in slightly better quality despite being almost imperceptible at times in a blind experiment. The results exhibit extremely plausible motion and are temporally stable. Subtle lip contact and stickiness is an issue but this affects manual tracking as well, hence the aforementioned additional deformations are applied after inference. The network produces perfectly stabilized vertex positions whereas human operators inevitably vary in their work between sequences. The results can also be improved by adding data to the training set if deemed necessary.

The 10 minute dataset requirement for high quality output means that the actor needs a big enough role in the game to justify the cost. Building the dataset for the neural network however enables tracking work to start prior to having a locked screenplay for the project. This means that late stage pick-up shoots and screenplay changes are much faster to deliver at a high quality. The dataset shoot allows the actor to familiarize himself with the script and the capture system and to work with the director to discover who the character is instead of practicing expressions just to cover facial muscle activations often with mixed results. Future work at Remedy will focus on capturing datasets using helmet-mounted cameras for true performance capture of the face and body simultaneously.

5.3 Perceptual loss function

In validation shots for which numerical quality results could be computed, the perceptual quality of network output did not always follow the value of the loss function. For example, a shot with low loss value might exhibit unnatural movement of lips or eyes, whereas a shot with a higher loss value may look more believable. In the latter case, the higher loss could often be explained by large skin areas being slightly offset tangentially, which is extremely difficult to spot as an artifact by a human observer. It was not always clear whether these errors were in the validation data or if the network output was amiss.

This suggests that it should be beneficial to design a more perceptually oriented loss function for facial expressions, similar in spirit to how structural similarity metrics have been developed for comparing images [Wang et al. 2004]. It seems clear that a better loss function would result in a more capable network, as it would learn to focus more on areas that require the highest precision. In our output, the vertex density is the highest around eyes and lips, which may already partially focus the attention of the network in this way, but nonetheless, a properly motivated perceptual loss function would be an interesting avenue for future work.

6 Conclusion

We have presented a neural network based facial capture method that has been found accurate enough to be applied in an upcoming game production based on thorough pre-production testing.

Even though the convolutional network may seem like an opaque building block, our approach retains all of the artistic freedom because we output simple 3D point clouds that can be further edited using standard tools, and compressed into standard character rigs. We feel that many other aspects of the production pipelines of modern games could benefit from similar, selective use of deep learning for bypassing or accelerating manual processing steps that have known but tedious or expensive solutions.

References

- BEELER, T., HAHN, F., BRADLEY, D., BICKEL, B., BEARDSLEY, P., GOTSMAN, C., SUMNER, R. W., AND GROSS, M. 2011. High-quality passive facial performance capture using anchor frames. *ACM Trans. Graph.* 30, 4, 75:1–75:10.

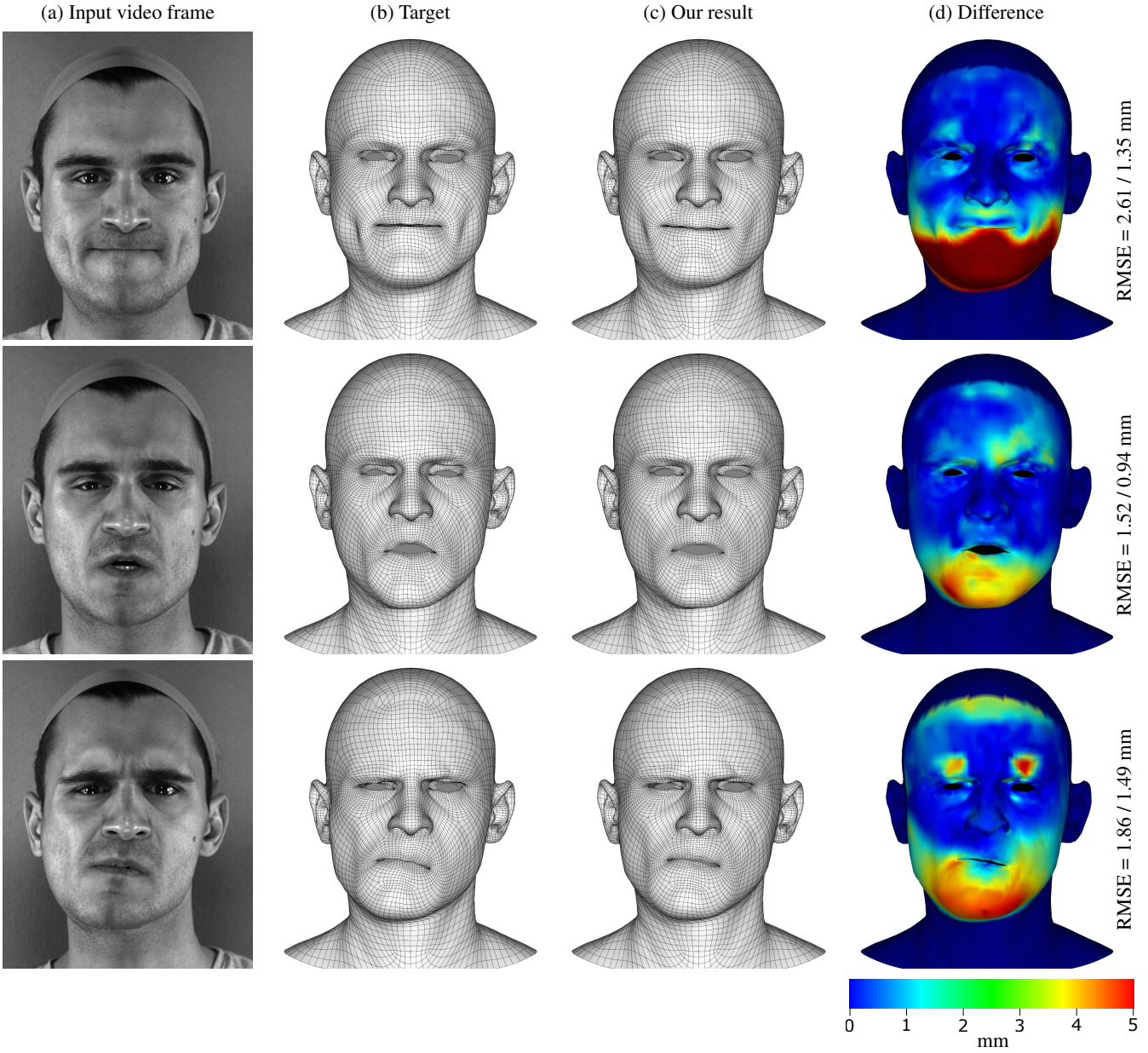


Figure 7: A selection of problematic frames where the neural network was unable to infer the position of the jaw accurately. The total error (first RMSE figure) is mostly in the direction perpendicular to the viewing direction (z) whereas the orthogonal (x, y) position of the jaw is captured reasonably well (second RMSE figure). With our current system, these depth estimation errors need to be manually corrected by the capture artists, but we expect that feeding the network a secondary input image, taken from the side, should solve these issues.

BENGIO, Y., LOURADOUR, J., COLLOBERT, R., AND WESTON, J. 2009. Curriculum learning. In *Proc. ICML*, 41–48.

CHUNG, M. K., 2012. Affine registration. <http://pages.stat.wisc.edu/~mchung/teaching/768/reading/lecture06-affine.pdf>.

COSTIGAN, T., PRASAD, M., AND McDONNELL, R. 2014. Facial retargeting using neural networks. In *Proc. MIG*, 31–38.

DENG, Z., CHIANG, P.-Y., FOX, P., AND NEUMANN, U. 2006. Animating blendshape faces by cross-mapping motion capture data. In *Proc. I3D*, 43–48.

DIELEMAN, S., SCHLÜTER, J., RAFFEL, C., OLSON, E., SØNDERBY, S. K., ET AL., 2015. Lasagne: First release.

DIMENSIONAL IMAGING, 2016. DI4D PRO System. <http://www.di4d.com/systems/di4d-pro-system/>.

FURUKAWA, Y., AND PONCE, J. 2009. Dense 3D motion capture for human faces. In *Proc. CVPR*.

FYFFE, G., HAWKINS, T., WATTS, C., MA, W.-C., AND DEBEVEC, P. 2011. Comprehensive facial performance capture. In *Computer Graphics Forum*, vol. 30, 425–434.

HE, K., ZHANG, X., REN, S., AND SUN, J. 2015. Delving deep into rectifiers: Surpassing human-level performance on imagenet classification. *CoRR abs/1502.01852*.

HINTON, G. E., SRIVASTAVA, N., KRIZHEVSKY, A.,

- SUTSKEVER, I., AND SALAKHUTDINOV, R. 2012. Improving neural networks by preventing co-adaptation of feature detectors. *arXiv preprint arXiv:1207.0580*.
- HONG, P., WEN, Z., AND HUANG, T. S. 2002. Real-time speech-driven face animation with expressions using neural networks. *IEEE Trans. on neural networks* 13, 4, 916–927.
- KAZEMI, V., AND SULLIVAN, J. 2014. One millisecond face alignment with an ensemble of regression trees. In *Proc. CVPR*.
- KINGMA, D. P., AND BA, J. 2014. Adam: A method for stochastic optimization. *CoRR abs/1412.6980*.
- KRIZHEVSKY, A., SUTSKEVER, I., AND HINTON, G. E. 2012. Imagenet classification with deep convolutional neural networks. In *Proc. NIPS*. 1097–1105.
- SIMARD, P. Y., STEINKRAUS, D., AND PLATT, J. 2003. Best practices for convolutional neural networks applied to visual document analysis. In *Proc. ICDAR*, vol. 3, 958–962.
- SIMONYAN, K., AND ZISSERMAN, A. 2014. Very deep convolutional networks for large-scale image recognition. *arXiv preprint arXiv:1409.1556*.
- SPRINGENBERG, J. T., DOSOVITSKIY, A., BROX, T., AND RIEDMILLER, M. A. 2014. Striving for simplicity: The all convolutional net. *arXiv preprint arXiv:1412.6806*.
- SRIVASTAVA, N., HINTON, G., KRIZHEVSKY, A., SUTSKEVER, I., AND SALAKHUTDINOV, R. 2014. Dropout: A simple way to prevent neural networks from overfitting. *Journal of Machine Learning Research* 15, 1929–1958.
- THEANO DEVELOPMENT TEAM. 2016. Theano: A Python framework for fast computation of mathematical expressions. *arXiv e-prints abs/1605.02688* (May).
- WANG, Z., BOVIK, A. C., SHEIKH, H. R., AND SIMONCELLI, E. P. 2004. Image quality assessment: From error visibility to structural similarity. *IEEE TIP* 13, 4, 600–612.
- WEISE, T., BOUAZIZ, S., LI, H., AND PAULY, M. 2011. Realtime performance-based facial animation. *ACM Trans. Graph.* 30, 4, 77:1–77:10.
- WILLIAMS, L. 1990. Performance-driven facial animation. *SIGGRAPH Comput. Graph.* 24, 4, 235–242.
- ZEILER, M. D., TAYLOR, G. W., SIGAL, L., MATTHEWS, I., AND FERGUS, R. 2011. Facial expression transfer with input-output temporal restricted boltzmann machines. In *Proc. NIPS*. 1629–1637.
- ZHANG, L., SNAVELY, N., CURLESS, B., AND SEITZ, S. M. 2004. Spacetime faces: High resolution capture for modeling and animation. *ACM Trans. Graph.* 23, 3, 548–558.
- A Appendix: Dealing with low-quality training data**
- Our initial training data was extracted from an older, massive facial motion database created using the conventional tracking pipeline. Despite the tracking artists' efforts to stabilize the facial mesh as part of the capture process, millimeter-scale inconsistencies remained between shots. This was problematic for training and validation, because the positional errors produced by the network were of similar magnitude. As a result, training could not progress beyond the point where the errors present in the training data started dominating the loss function. Experimenting with different network architectures, etc., was difficult, as most networks could reach this plateau and hence the numerical results always ended up looking similar.
- In order to make progress, we devised two techniques for coping with the stabilization errors in the vertex positions in the training data. The first one was using affine transform invariant loss function for training and validation, and the second was performing additional per-shot mesh stabilization as a pre-process.
- As the project progressed to the point of evaluating the feasibility of producing a single, well-curated training set for each actor, it became possible to improve the quality of input by having the tracking artists pay especially close attention to the problematic areas, including head stabilization.
- A.1 Affine-invariant loss function**
- A natural choice for loss function is the mean square distance between the predicted vertex positions and the target positions in the training data. However, as explained above, this leads to problems because the target positions do not necessarily represent a ground truth result due to stabilization errors.
- As an attempt to remove the effect of stabilization errors on the loss, we experimented with a loss function that is invariant to affine transformations between the predicted positions and the target positions. To achieve this, the loss function first finds the L_2 -optimal affine transformation between the predicted positions and the target positions, and then takes the mean square error between the predicted positions taken through this transform and the target positions.
- The predicted positions, transformed with the L_2 -optimal affine transform [Chung 2012], can be calculated as:
- $$P' = P((Q^T P)(P^T P)^{-1})^T,$$
- where P is a $n \times 4$ matrix whose rows contain the coordinates of each predicted position padded with a 1, i.e., $(x, y, z, 1)$, Q is a similar matrix containing the target positions, and P' receives the transformed predicted positions. Note that $P^T P$ is always a 4×4 matrix, so the required matrix inversion is easy to compute analytically. The final loss is then $\frac{1}{n} \sum [(P' - Q)^2]$, where the squaring is done per-element, and the sum is taken over all elements. As the rightmost column of P' is always ones (up to arithmetic precision), it does not contribute to the loss, and calculating it can be skipped.
- Note that it is crucial that we determine the affine transformation from predicted positions to target positions, instead of vice versa. If we allowed an affine transformation to be applied to the target positions before evaluating the MSE, the network would recognize that simply outputting a smaller mesh produces smaller post-transformation error. In the limit, placing all output positions in the same position would result in zero loss.
- Problems.** The affine-invariant loss function removes the effects of stabilization errors on the loss, but it was found to have severe negative consequences, as it removes any encouragement for the network to produce the output in a fixed position, size, or orientation. If employed in production, this would necessitate post-process stabilization of the inferred results, which is undesirable.
- If we make the output layer weights fixed—corresponding to the network outputting PCA coefficients, as explained in Section 3.1—the affine-invariant loss function works fine, as the fixed PCA basis at the output prevents spurious movement of the output mesh. This, however, prevents training the output layer weights, which is not optimal. Moreover, the output PCA acts as such a strong prior for the network that the results are practically identical to using the standard loss function.

A.2 Pre-process mesh stabilization

Our second attempt to deal with stabilization errors in the target positions was to run an additional stabilization pass on the training data. Our ad-hoc shot stabilization method works as follows. First we compute, for each frame of the shot, the mean squared distance between the target point set and the rest pose, and sort the frames according to this metric. Then we select 50% of the frames that had the smallest difference to the rest pose, with the goal of avoiding frames where the face differs significantly from the rest pose. After this, we find a single affine transformation that minimizes the mean Euclidean distance between the target point sets in the chosen frames and the rest pose. This L_1 -optimal transformation is computed using iterative gradient descent.

This approach allows keeping the output layer weights trainable, but it cannot account for drift or non-affine shape errors in the shot. However, it allowed us to progress forward with the development of the network architectures and training methods, and was consistently used until higher-quality training datasets became available.

A.3 Discussion

We currently employ neither of these techniques during training, validation, or inference, because the training data made for production use is sufficiently well stabilized. As mentioned above, affine-invariant loss function forbids training of the output layer, and performing additional stabilization to already stable vertex positions can only make the situation worse. Hence not touching the data at all is the best we can do. However, when experimenting with less than perfectly stabilized vertex data, we found the techniques described above useful, and therefore chose to include them in this appendix for the benefit of those in a similar situation.

B Appendix: Fully connected network

When experimenting with fully connected networks, we achieved the best results by transforming the input images into 3000 PCA coefficients. The PCA basis is pre-calculated based on the input frames from the training set, and the chosen number of basis images captures approximately 99.9% of the variance in the data. The layers of the network are listed in the table below.

Name	Description
input	Input 3000 image PCA coefficients
fc1	Fully connected 3000 → 2000, ReLU activation
drop1	Dropout, $p = 0.2$
fc2	Fully connected 2000 → 1000, tanh activation
drop2	Dropout, $p = 0.2$
fc3	Fully connected 1000 → 160, linear activation
output	Fully connected 160 → N_{out} , linear activation

The position and the orientation of the head in the input images varies, which in practice necessitates stabilizing the input images prior to taking the PCA transformation. For this we used the facial landmark detector of Kazemi and Sullivan [2014], an implementation of which can be found in the `dlib` machine learning package. Rotation angle and median line of the face were estimated from the landmark points surrounding the eyes. Because these were found to shift vertically during blinking of the eyes, the vertical position of the face was determined from the landmark points on the nose. The image was then rotated to a fixed orientation, and translated so that the point midway between the eyes remained at a fixed position.

Even though the network may seem overly simplistic, we did not find a way to improve the results by adding more layers or changing

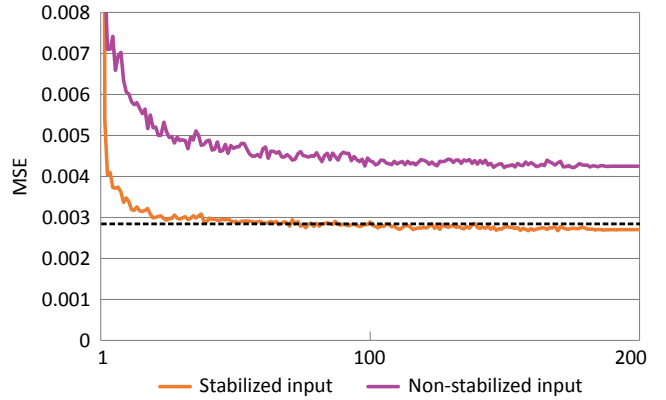


Figure 9: Convergence of the validation loss of the fully-connected network. The training took approximately one hour, and the training set was the same as for Figure 8. The dashed horizontal line shows the converged validation loss of the convolutional network, and we can see that with stabilized input images, the fully connected network reaches slightly smaller loss. However, the results were perceptually clearly inferior. Using non-stabilized input images yielded much worse results both numerically and perceptually.

the widths of the existing layers. We experimented with different regularization schemes, but simply adding two dropout layers was found to yield the best results. The output layer is initialized using a PCA basis for the output meshes computed as in the convolutional network (Section 3.1).

B.1 Comparison

Ultimately, the only aspect in which the fully connected network remained superior to the convolutional network was training time. Whereas the convolutional network takes 8–10 hours to train in a typical case, the fully connected network would converge in as little as one hour. Even though it was initially speculated that fast training times could be beneficial in production use, it ended up not mattering much as long as training could be completed overnight.

Stabilizing the input images for the fully connected network turned out to be problematic because of residual motion that remained due to inaccuracies in the facial landmark detection. This residual jitter of input images sometimes caused spurious and highly distracting motion of output vertices. We tried hardening the fully connected network to this effect by applying a similar jitter to inputs during training, i.e., presenting the same stabilized input image to the network in slightly different positions, but this did not help.

We suspect that it may be too difficult for the fully connected network to understand that slightly offset images should produce the same result, perhaps partially due to the input PCA transform. Nonetheless, the results with input PCA transform were better than using the raw image as the input. The convolutional network does not suffer from these problems, as input image stabilization is not required.

The fully connected network often produced numerically better results than the convolutional network (Figure 9), but perceptually the results were significantly worse, as the fully connected network appeared to generally attenuate the facial motion. Even in individual shots where the fully connected network produced a numerically clearly superior result, the facial motion was judged to lack expressivity and was not as temporally stable compared to the results produced by the convolutional network.